

Supporting Information

Smart nanopaper sensor for optical diagnosis of *Helicobacter pylori* infection

Zeinab Asghari Adib¹, Amir Reza Sharifi¹, Mohammad Ali Kiani¹, Hossein Yousefi², Daniel Horák³,
Uliana Kostiv³, Ali Nabavi-Rad⁴, Abbas Yadegar⁴, Mohammad Yaghoubi-Avini⁵, and Hamed
Golmohammadi^{1,6*}

¹ Nanosensor Bioplatfroms Laboratory, Chemistry and Chemical Engineering Research Center of Iran, 14335-186, Tehran, Iran.

² Laboratory of Sustainable Nanomaterials, Department of Wood Engineering and Technology, Gorgan University of Agricultural Sciences and Natural Resources, Gorgan, 4913815739, Iran.

³ Institute of Macromolecular Chemistry, Academy of Sciences of the Czech Republic, Heyrovského nám. 2, 162 06 Prague 6, Czech Republic.

⁴ Foodborne and Waterborne Diseases Research Center, Research Institute for Gastroenterology and Liver Diseases, Shahid Beheshti University of Medical Sciences, Tehran, Iran.

⁵ Departments of Microbiology and Microbial Biotechnology, Faculty of Life Sciences and Biotechnology, Shahid Beheshti University G.C., Tehran, Iran.

⁶ Department of Microsystems Engineering (IMTEK), University of Freiburg, 79110 Freiburg, Germany.

* Corresponding author email: hamed.golmohammadi@imtek.uni-freiburg.de

golmohammadi@ccerci.ac.ir

Table of Contents

Characterization of chitin nanofiber (ChNF) and nanopaper (ChNP)	S3
Instrumentation	S3
Results	S4
Figure S1. The FT-IR spectrum of the produced ChNP.....	S4
Figure S2. AFM micrograph of ChNP produced with super disk grinder and its diameter distribution.....	S5
Figure S3. FE-SEM micrographs of ChNP: a) Surface and b) tensile-broken surface.	S5
Figure S4. The XRD curve of the produced ChNP: a) XRD curve of ChNP b) 2D-WAXS pattern and image at edge and b) through directions of the ChNP. The value of crystallite orientation (π) of each specimen was mentioned in percent.	S6
Figure S5. A comparison among the specific tensile strengths of the ChNP made in this study with those of paper ² , high-density fiberboard (HDF), medium density fiberboard (MDF), wood plastic composite (WPC; PP + 40% wood flour + 3% coupling agent), particleboard (PB), steel (structural ASTM A36 steel), polypropylene (PP), high-density polyethylene (HDPE) and polyvinyl chloride (PVC) ⁴	S7
Figure S6. The tensile stress-strain curve of the produced ChNP.	S8
Table S1. Estimated cost of the developed nanosensor and the fabricated portable imaging platform (SIS).....	S8
Reference:	S9

Characterization of chitin nanofiber (ChNF) and nanopaper (ChNP)

Instrumentation

FT-IR analysis was carried out by INVENIO FT-IR Spectrometer, Bruker, Germany. Atomic force microscope (SII Nanonavi E-sweep; SII Nanotechnology, Inc., Japan) in a dynamic force mode was used to record AFM micrographs of ChNF. The AFM probe was made of Si with a spring constant of 18 N/m and a frequency of 138 kHz. The average diameter of ChNFs was also measured using a Digimizer (MedCalc Software Co.). A field emission scanning electron microscopy (FE-SEM), (Sigma 300-HV; Zeiss, Germany) at an accelerating voltage of 5 kV was employed for the observation of specimens. All specimens were dried in vacuum and deposited with gold (DSR1; desk sputter coater, Nanostructured Coatings co., Iran). The diameters of 300 micro- and nanofibers were measured on micrographs using ImageJ software. An X-ray diffraction test was carried out using a Bruker D8 Advance (Bruker Co., USA). The specimens were irradiated by $\text{CuK}\alpha$ radiation at 35 kV and 35 mA, in the range of $2\theta = 10\text{-}40^\circ$ at a scanning speed of $1.2^\circ/\text{min}$.

The Crystallinity index (*CrI*) was evaluated using the following equation.¹

$$CrI = \frac{100(I - I_a)}{I} \quad (1)$$

Where I is the maximum diffraction intensity of ChNF, I_a is the intensity measured at 2θ of 16 degrees, where the maximum occurs in a diffractogram for non-crystalline chitin.

The crystallite orientation (π) was determined by the following equation for the azimuthal profile of the 200 reflection appeared at 2D wide angle X-ray scattering (2D-WAXS) pattern.²

$$\pi = 180 - H/180 \quad (2)$$

where H is the full width at the half maximum along the Debye-Scherrer ring.

The tensile test of ChNP was performed with a universal material testing machine (MP48A 20, Iran) equipped with a 100 N load cell. The specimens were cut into thin strips with a specimen width of 5 mm and were dried in vacuum oven prior to test. For the tensile testing, a 60-mm gauge length was set under a strain rate of 5 mm/min and 10 specimens were measured.

Results

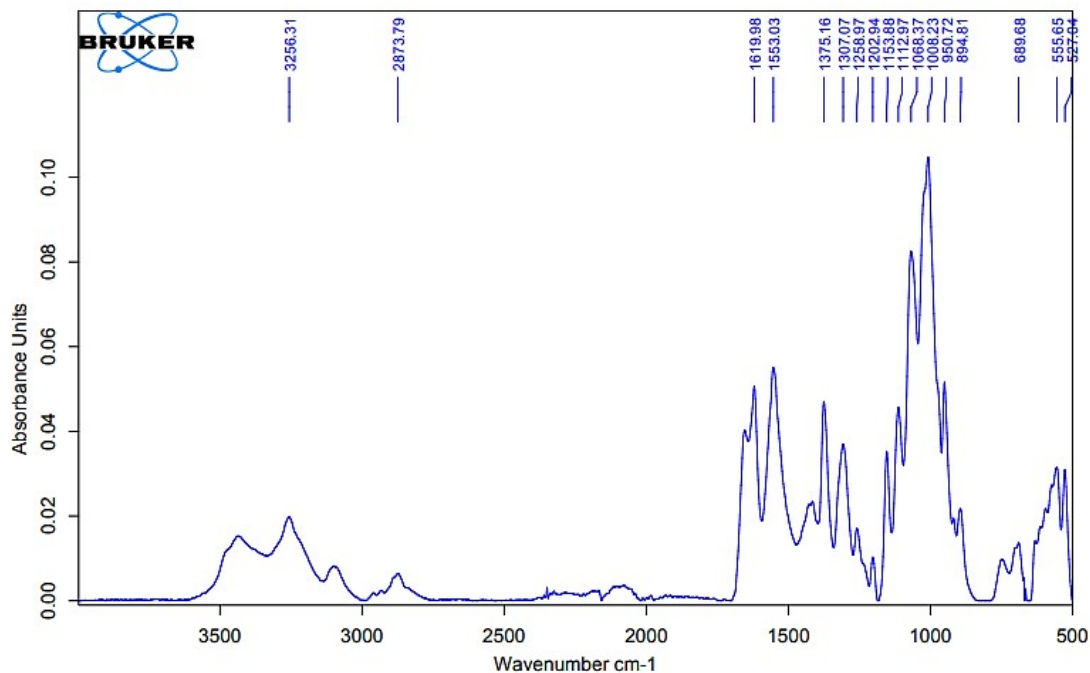


Figure S1. The FT-IR spectrum of the produced ChNP.

Figure S2 shows AFM micrograph of ChNP produced with super disk grinder and diameter distribution of prepared ChNF. The purified chitin was downsized to nanofibers with diameters ranging from 5-55 nm (average: 26 ± 8 nm), as the result of pressure and shearing forces created between the grinder disks. These sizes are almost in the range of chitin and cellulose nanofibers produced with disk grinder.

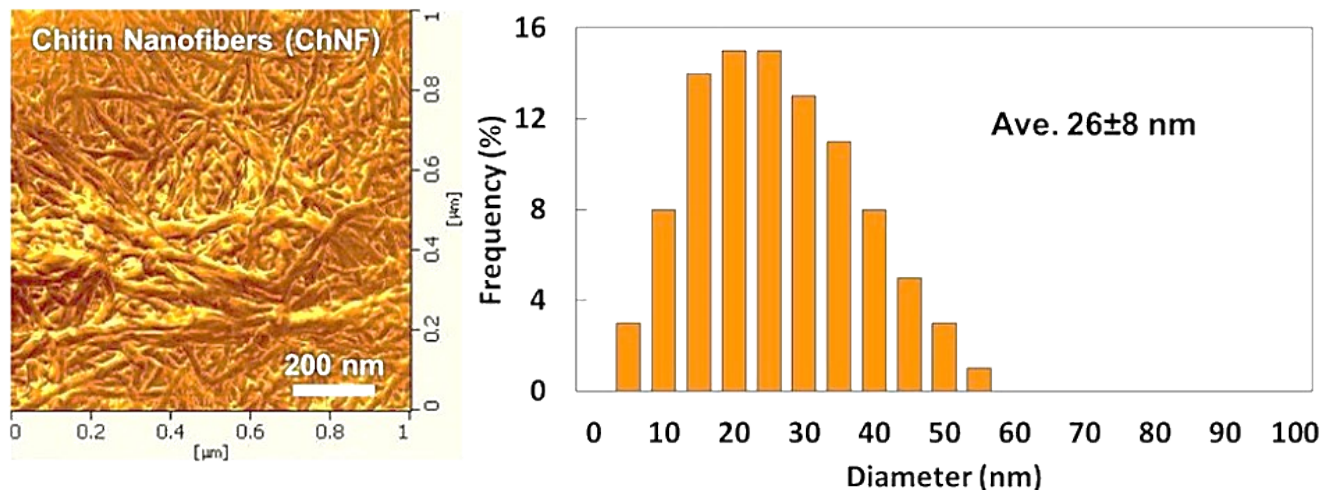


Figure S2. AFM micrograph of ChNP produced with super disk grinder and its diameter distribution.

Figure S3 shows the FE-SEM micrographs of ChNP: a) Surface and b) tensile-broken surface. The nanofibers with diameters ranging from 5-45 nm (average: 26 ± 8 nm) were detected in the micrographs. This downsizing was carried out as the result of pressure and shearing forces created between the grinder disks.

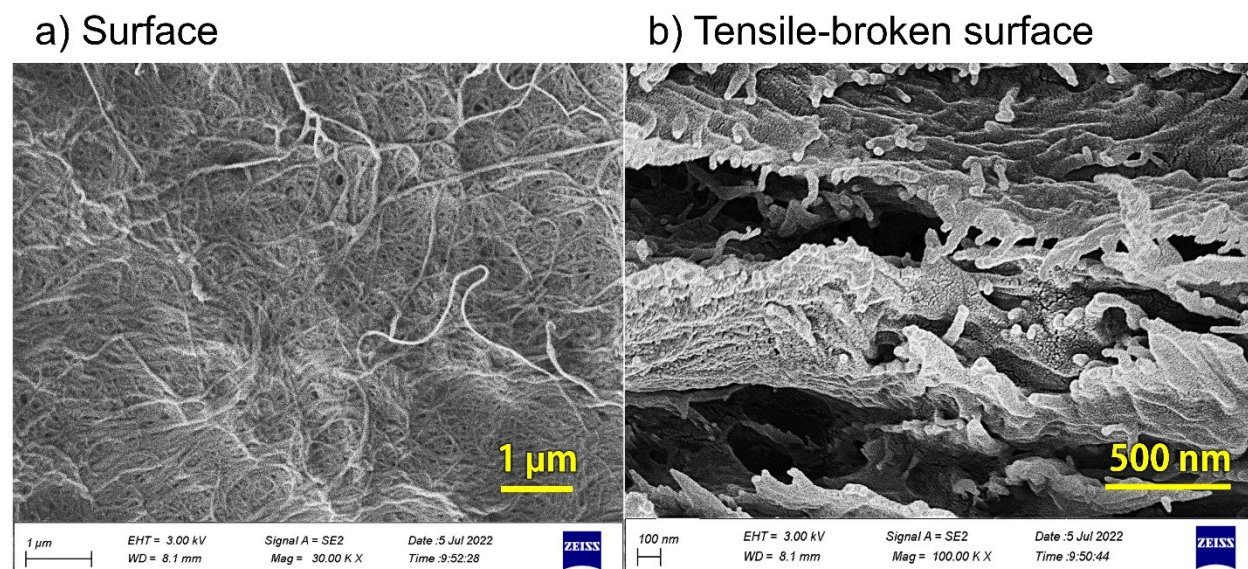


Figure S3. FE-SEM micrographs of ChNP: a) Surface and b) tensile-broken surface.

Figure S4a depicts the XRD curve of ChNP which showed peaks at 2θ of 9.5, 21 and 23.5 degrees and a crystallinity index of 89%. This confirms that ChNF is a high crystalline material with a crystallinity index higher than that of wood-driven cellulose nanofibers. Figures S4b and S4c depict the 2D-WAXS pattern and image at two direction of edge (b) and through (c) of the ChNP, together with their corresponding π -value (crystallite orientation) of the diffraction for the 200 reflection along the Debye-Scherrer ring. The Debye-Scherrer rings in the through-irradiated

specimens showed a constant equatorial distribution scattering intensity with a π -value of zero. This corresponds to a random in-plane distribution of the ChNFs, which is in agreement with FE-SEM micrograph as shown in Figure S3. In the case of edge-irradiated specimens, they presented a not constant equatorial distribution scattering intensity, resulted in a π -value of 78%. This result confirmed the laminate structure of nanopaper and its in-plane isotropic structure.

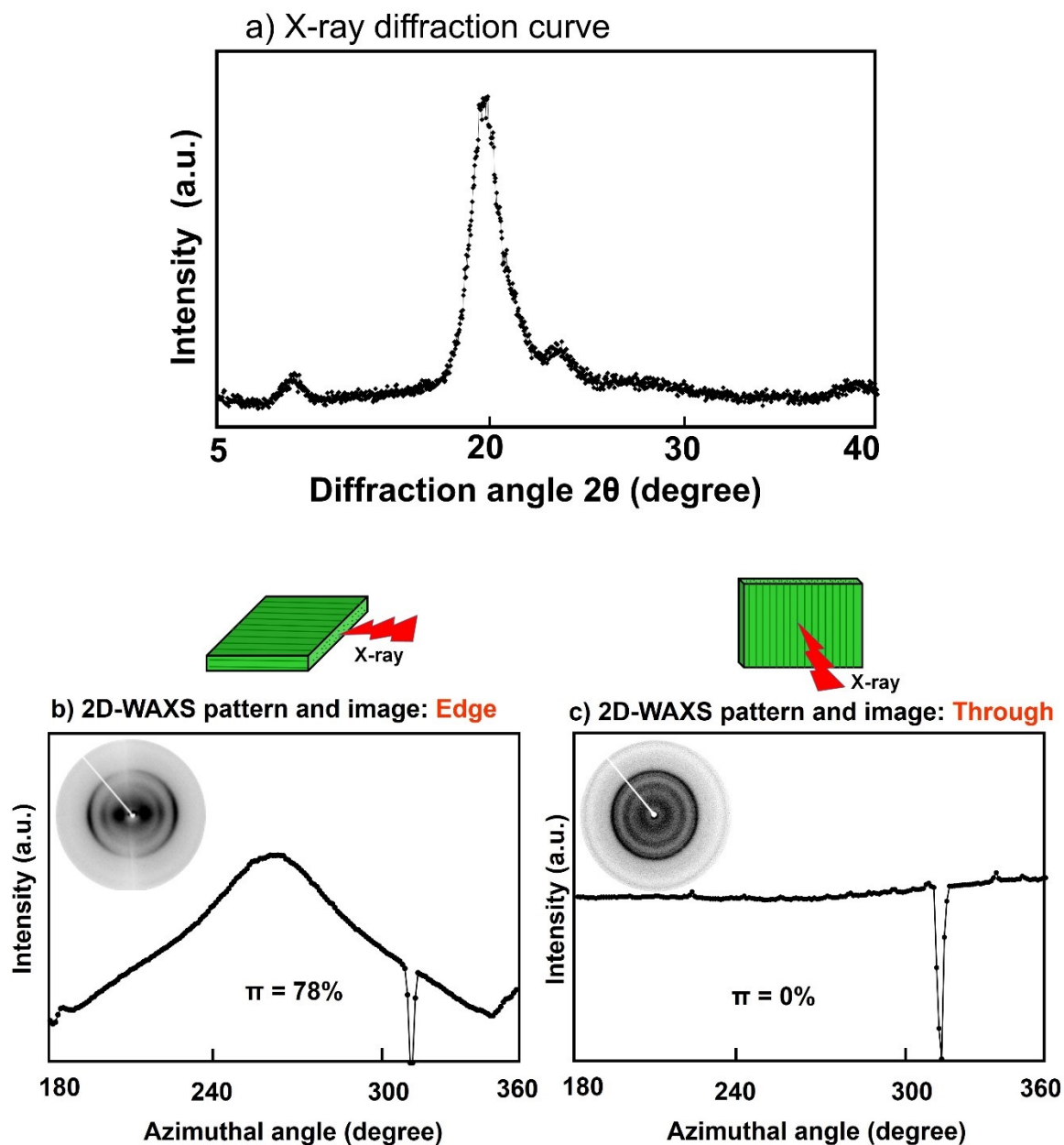


Figure S4. The XRD curve of the produced ChNP: a) XRD curve of ChNP b) 2D-WAXS pattern and image at edge and b) through directions of the ChNP. The value of crystallite orientation (π) of each specimen was mentioned in percent.

Figure S5 shows a comparison among the specific tensile strengths of the ChNP made in this study with those of paper² high-density fiberboard (HDF), medium density fiberboard (MDF), wood plastic composite (WPC; PP + 40% wood flour + 3% coupling agent), particleboard (PB), steel (structural ASTM A36 steel), polypropylene (PP), high-density polyethylene (HDPE) and polyvinyl chloride (PVC).³ The tensile strength, young's modulus and stain at break of ChNP obtained were 176 MPa, 9.5 GPa and 8.6%, respectively. The specific tensile strengths obtained by dividing corresponding tensile strengths to the specific gravity of the mentioned materials. As it can be seen, the specific tensile strength of ChNP is much higher than that of other specimens even with that of steel. This is mainly because of high specific surface area, network structure, high crystallinity of ChNP as well as its relative low density (1.4 g/cm³). Also, ChNP is fully made of bio-based nanofibers with no synthetic resin/additives; hence, it is regarded as fully environmentally friendly material.

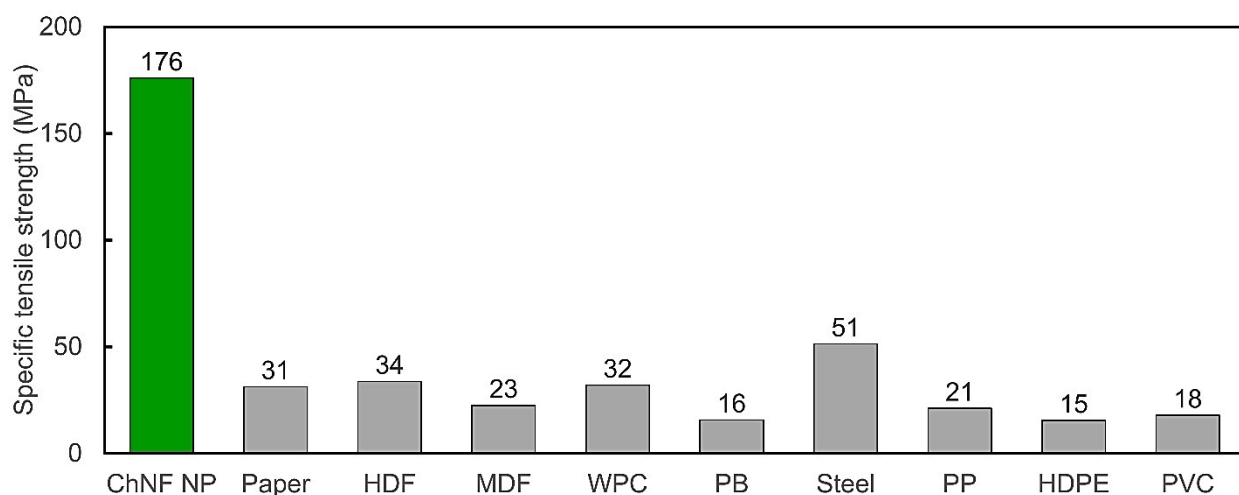


Figure S5. A comparison among the specific tensile strengths of the ChNP made in this study with those of paper², high-density fiberboard (HDF), medium density fiberboard (MDF), wood plastic composite (WPC; PP + 40% wood flour + 3% coupling agent), particleboard (PB), steel (structural ASTM A36 steel), polypropylene (PP), high-density polyethylene (HDPE) and polyvinyl chloride (PVC)³.

Figure S6 depicts the tensile stress-strain curve of ChNP. The tensile strength, Young's modulus and strain at break of ChNP obtained were 135 MPa, 7.7 GPa and 8.2%, respectively. The results are compatible with those in the literature.^{4, 5}

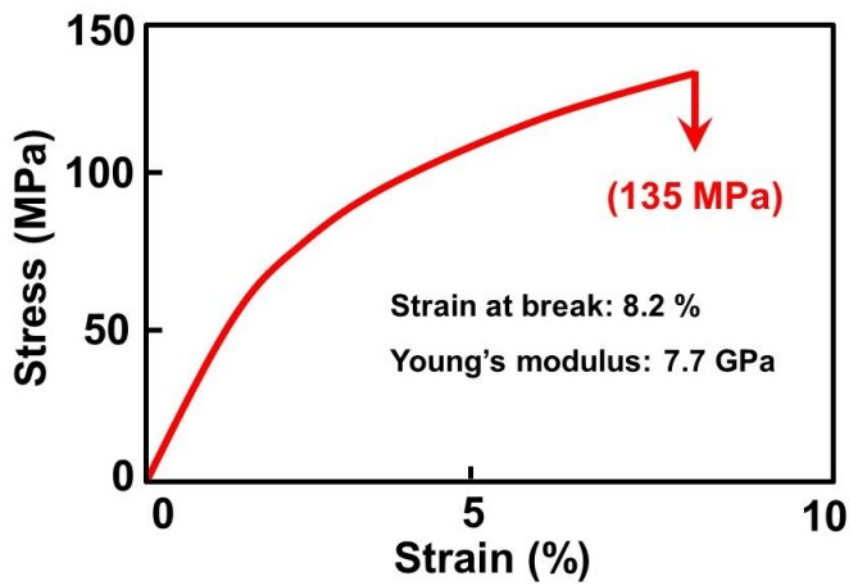


Figure S6. The tensile stress-strain curve of the produced ChNP.

Table S1. Estimated cost of the developed nanosensor and the fabricated portable imaging platform (SIS)

Material	Stock Volume/Amount	Price (\$)	Volume/Amount required for each patch	Price for each patch (\$)
Chitin nanopaper (ChNP)	1 sheet (1m ²)	20	3 × 28.9 mm ²	~ 0.002
Upconversion nanoparticles (UCNPs)	5 ml	50	0.3 μl	~ 0.003
Red cabbage extract	200 ml	5	7.7 μl	~ 0.0002
FeCl ₂ ·4H ₂ O	250 g	40	2 mg	~ 0.0003
FeCl ₃ ·6H ₂ O	250 g	24	1 mg	~ 0.0000
Ammonia solution (25%)	500 ml	7.6	100 μl	~ 0.0015

Total ~0.007

SIS components	Price (\$)
Infrared laser diode module	~ 200
Optical ultra-violet (UV)/near-infrared (NIR) cut-off filter	~ 10
Glass strip/slide	~ 1
Plastic and bolt/nut	~ 5
Total	~ 216

Reference:

1. M. K. Jang, B. G. Kong, Y. I. Jeong, C. H. Lee and J. W. Nah, *J. Poly. Sci. Part A: Poly. Chem.*, 2004, **42**, 3423-3432.
2. H. Yousefi, M. Faezipour, T. Nishino, A. Shakeri and G. Ebrahimi, *Polym. J.*, 2011, **43**, 559-564.
3. Z. Cai and R. J. Ross, *Wood handbook-Wood as an engineering material. Centennial edition. General Technical Report FPL-GTR-190. Department of Agriculture, Forest Service, Forest Products Laboratory. Madison, Wisconsin, EUA*, 2010, **12**.
4. W. Huang, in *Nanopapers*, Elsevier, 2018, pp. 175-200.
5. Y. Fan, H. Fukuzumi, T. Saito and A. Isogai, *Int. J. Biol. Macromol.*, 2012, **50**, 69-76.